



ChemComm

**Novel Method for Preparing Stable Near-Infrared Absorbers:
New Phthalocyanine Family based on Rhenium(I)
Complexes**

Journal:	<i>ChemComm</i>
Manuscript ID	CC-COM-07-2020-004625.R1
Article Type:	Communication

SCHOLARONE™
Manuscripts

COMMUNICATION

Novel Method for Preparing Stable Near-Infrared Absorbers: New Phthalocyanine Family based on Rhenium(I) Complexes

Kei Murata,^a Yosuke Koike^a and Kazuyuki Ishii^{*a}

Received 00th January 20xx,
Accepted 00th January 20xx

DOI: 10.1039/x0xx00000x

Reasonable design of near-infrared (NIR) absorbing molecules is crucial for developing photofunctional materials. Here, we synthesized dinuclear and mononuclear Re(I) tricarbonyl phthalocyanine complexes that exhibit a sharp intense Q band in the NIR region. Unsymmetric coordination of the electron-deficient metal unit(s) concomitantly produced a remarkable red shift of the Q band and improved the tolerance of the phthalocyanine ring to oxidation. This study presents a simple effective strategy for construction of NIR absorbers with high stability.

Red or near-infrared (NIR) light absorbing molecules are widely used as dyes, pigments, luminescent materials,

photocatalysts, and photosensitizers for solar energy devices.¹ In addition, absorption in the red or NIR region is particularly attractive from the viewpoint of biological applications, such as photodynamic therapy and photothermal therapy, because it corresponds to a major part of the biological window.² Phthalocyanine (Pc) derivatives are often incorporated into these materials because they exhibit intense absorption bands (Q bands) in the red and/or NIR regions. In typical diamagnetic Pcs, the Q band originates from electronic transitions from the singlet ground (S_0) state to the lowest excited singlet (S_{1x} and S_{1y}) states, which are mainly composed of the HOMO \rightarrow LUMO/LUMO+1 properties is crucial for tuning the electronic states of the Pc ring.

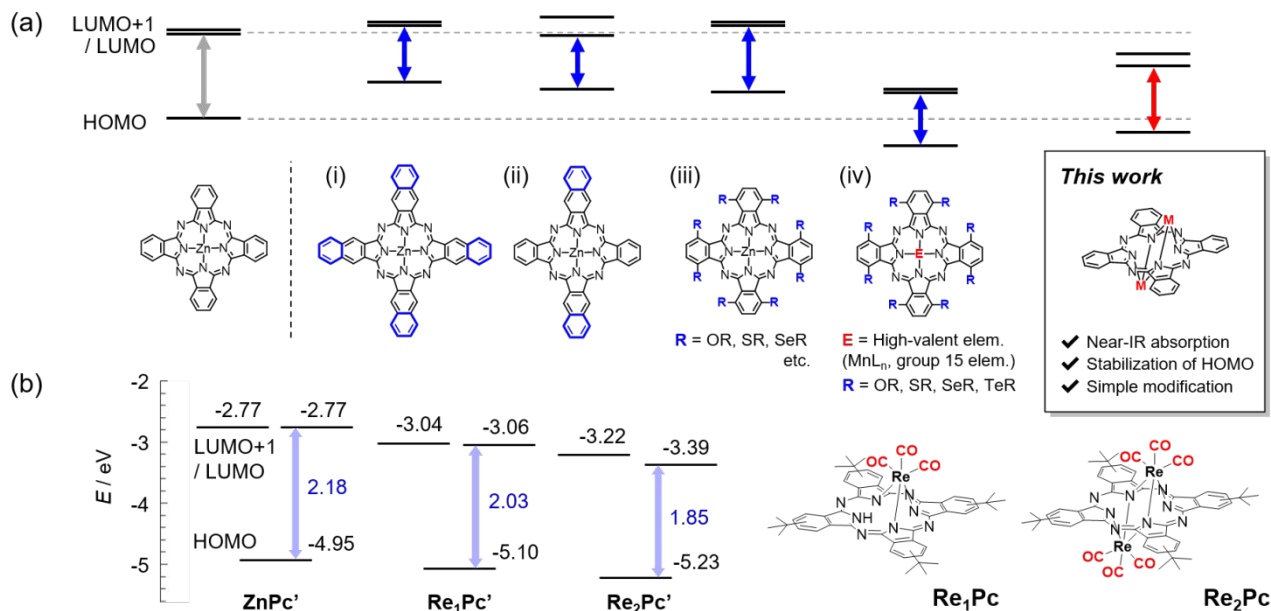


Fig. 1 (a) Schematic representation of the strategies for controlling frontier orbitals of Pcs and (b) Structures of **Re₁Pc** and **Re₂Pc** and the frontier molecular orbital energy diagrams of the model complexes (**Re₂Pc'**, **Re₁Pc'** and **ZnPc'**) based on DFT (B3LYP / LanL2DZ (for Re) and 6-31G(d,p) (for other atoms).

^a Institute of Industrial Science, The University of Tokyo, 4-6-1 Komaba, Meguro-ku, Tokyo 153-8505, Japan.

E-mail: k-ishii@iis.u-tokyo.ac.jp

† Electronic Supplementary Information (ESI) available: Experimental details, spectroscopic observations, electrochemistry, tolerance to oxidation and DFT analyses. See DOI: 10.1039/x0xx00000x

To develop Pc chromophores possessing a lowered Q band energy, a variety of molecular designs for decreasing the HOMO–LUMO gap have been proposed.³ One typical strategy is to expand the π -conjugated system of the Pc ring (Fig. 1a (i)). Based on this concept, various naphthalocyanines and

anthracocyanines have been synthesized, and their photophysical properties have been investigated.⁴ Fusion of aromatic units onto the Pc rings generally destabilizes both the HOMO and LUMO/LUMO+1 energy levels, and it reduces the HOMO–LUMO gap based on the larger destabilization of the HOMO energy level. Lowering the symmetry of the π -conjugated system also reduces the HOMO–LUMO gap. For unsymmetric fusion of aromatic units, the degeneracy of the LUMO and LUMO+1 is lifted, in addition to destabilization of the HOMO energy level (Fig. 1a (ii)).⁵ Another strategy is to introduce electron-donating groups (e.g., $-\text{NR}_2$, $-\text{OR}$, $-\text{SR}$, $-\text{SeR}$, and $-\text{TeR}$) on the α -positions of the Pc rings, which also reduces the HOMO–LUMO gap because of the large HOMO distributions on the α -positions (Fig. 1a (iii)).⁶ Introduction of bulky groups on the α -positions induces distortion of the Pc rings, resulting in a similar effect.⁷ However, these strategies involving destabilization of the HOMO level often decrease the stability in terms of the tolerance to oxidation, which is one of the most important parameters for stability in air.⁸ An alternative approach is to use a high-valent central element. For example, Mn(III) is effective for decreasing the HOMO–LUMO gap with HOMO stabilization (Fig. 1a (iv)).⁹ Furthermore, the combination of a high-valent, group 15 element (P(V), As(V), or Sb(V)) and strong electron-donating substituents on the α -positions of a Pc ring substantially decreases the HOMO–LUMO gap and the Q band energy.¹⁰ However, this strategy generally requires complex modification of the ring, and it is therefore still challenging to develop a novel simple approach for preparing stable Pcs with highly lowered Q band energy.

In this study, we developed a series of Re(I) tricarbonyl Pc complexes that exhibit sharp intense absorption bands in the NIR region (Fig. 2). The Q bands of the complexes substantially shifted to the lower energy side by unsymmetric coordination of the Re(I) tricarbonyl unit(s) without introducing special substituents to the macrocycle. Both experimental and theoretical studies indicated that the HOMO–LUMO gap significantly decreased by both stabilizing the HOMO and LUMO/LUMO+1 levels and lifting the degeneracy of the LUMO and LUMO+1. This strategy provides a simple effective approach for constructing Pc-based NIR absorbers with high stability.

The dinuclear complex (tetra-*tert*-butylphthalocyaninato)-bis(tricarbonyl rhenium (I)) (**Re₂Pc**) was synthesized by the metal insertion reaction into tetra-*tert*-butyl-29H,31H-phthalocyanine using dirhenium(I) dodecacarbonyl as the Re(I) source. Interestingly, **Re₂Pc** caused a partial demetallation reaction to selectively give the mononuclear complex (tetra-*tert*-butylphthalocyaninato)tricarbonyl rhenium(I) (**Re₁Pc**) by treating with a coordinative solvent, such as pyridine or methanol. Direct clean conversion of **Re₂Pc** to **Re₁Pc** was confirmed by electronic absorption spectroscopy (Fig. S1). The isolated complexes were sufficiently stable in air, and they were characterized by elemental analysis and several spectroscopic methods. In the Fourier transform infrared (FT-IR) spectra, multiple intense bands were observed in the CO stretching region for both **Re₂Pc** (1916 and 2026 cm^{-1}) and **Re₁Pc** (1908 and 2022 cm^{-1}) (Figure S2). In the ¹H NMR spectrum of **Re₁Pc**, a signal attributed to a pyrrole proton on the Pc ring was observed, which

was not observed for **Re₂Pc**. These results indicated that one and two $[\text{Re}(\text{CO})_3]^+$ units were attached to the Pc ring instead of pyrrole protons for **Re₁Pc** and **Re₂Pc**, respectively, which are different from the previously reported Pc complexes possessing an oxo, nitrosyl, nitrido, or organoimido rhenium center.¹¹

Electronic absorption and magnetic circular dichroism (MCD) spectra of **Re₂Pc**, **Re₁Pc**, and zinc(II) tetra-*tert*-butylphthalocyanine (**ZnPc**) are shown in Fig. 2a and b. **Re₂Pc** and **Re₁Pc** in toluene exhibit intense Q bands at 798 and 745 nm, respectively, which are attributed to the π - π^* transitions based on the time-dependent DFT (TD-DFT) calculations (vide infra). The Q band substantially shifts to the lower energy side as the number of $[\text{Re}(\text{CO})_3]^+$ units increase ($\Delta\lambda_{\text{max}}$ with respect to the Q band of **ZnPc**: 65 nm for **Re₁Pc** and 118 nm for **Re₂Pc**). These shifts are much larger than those of Pcs possessing high-valent central elements (λ_{max} in CHCl_3 : 730 nm for $\text{MnClPc}^{\text{tBu}}$ and 716 nm for $\text{P}(\text{OMe})_2\text{Pc}^{\text{tBu}}$).^{10b} In addition, introduction of the $[\text{Re}(\text{CO})_3]^+$ unit(s) considerably broadens the absorption band (full width at half maximum: 450 cm^{-1} for **ZnPc**, 780 cm^{-1} for **Re₁Pc**, and 830 cm^{-1} for **Re₂Pc**) with decreasing extinction coefficient at the maximum ($\epsilon = 2.9 \times 10^5 \text{ M}^{-1} \text{ cm}^{-1}$ for **ZnPc**, $\epsilon = 1.1 \times 10^5 \text{ M}^{-1} \text{ cm}^{-1}$ for **Re₁Pc**, and $\epsilon = 7.2 \times 10^4 \text{ M}^{-1} \text{ cm}^{-1}$ for **Re₂Pc**). In the shorter wavelength region (300–450 nm), for **Re₂Pc** and **Re₁Pc**, the B bands also shift to the lower energy side. Further, the additional, broad absorption bands are seen in 550–600 nm region ($\lambda_{\text{max}} \sim 560 \text{ nm}$ for **Re₁Pc**, 600 nm for **Re₂Pc**), which are attributed to the metal-to-ligand charge transfer (MLCT) transitions based on the TD-DFT calculations (vide infra). In the MCD spectra, dispersion-type spectral patterns in the Q-band region are observed for **Re₁Pc** and **Re₂Pc**.¹² Peak splitting of the positive/negative signal increases by the introduction of $[\text{Re}(\text{CO})_3]^+$ units ($\Delta\lambda_{\text{pos/neg}} = 11 \text{ nm}$ for **ZnPc**, $\Delta\lambda_{\text{pos/neg}} \sim 25 \text{ nm}$ for **Re₁Pc**, and $\Delta\lambda_{\text{pos/neg}} \sim 22 \text{ nm}$ for **Re₂Pc**). Thus, in contrast to the Faraday *A* term observed for **ZnPc**, the MCD spectral patterns for **Re₁Pc** and **Re₂Pc** are attributed to the quasi-Faraday *A* term. These results indicated that the Pc skeletons in **Re₁Pc** and **Re₂Pc** significantly deviated from *D*_{4h}

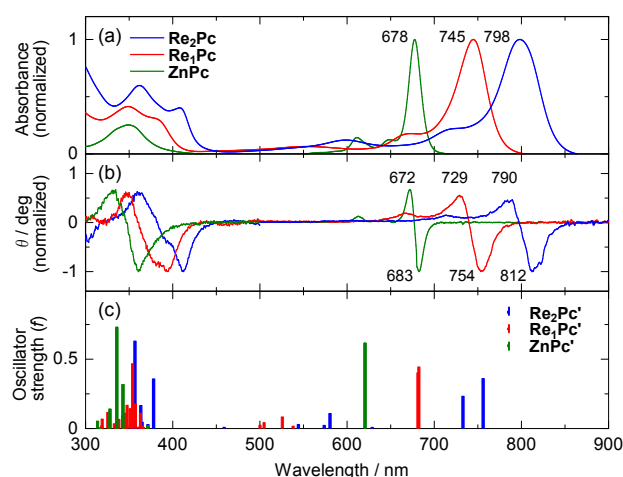


Fig. 2 (a) Electronic absorption and (b) MCD (b, < 500 nm: $\text{Abs}(\text{Q}_{\text{max}}) = 1.0$, > 500 nm: $\text{Abs}(\text{B}_{\text{max}}) = 1.5$, experimental details are described in ESI) spectra of **Re₂Pc** (blue), **Re₁Pc** (red) and **ZnPc** (green). (c) Calculated electronic transitions of the excited singlet states of the model complexes (**Re₂Pc**^{*}, **Re₁Pc**^{*} and **ZnPc**^{*}) based on TD-DFT (B3LYP / LanL2DZ (for Re) and 6-31G(d,p) (for other atoms) with PCM (toluene)).

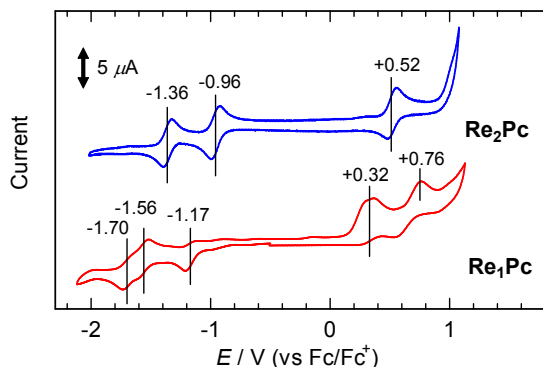


Fig. 3 Cyclic voltammograms of **Re₂Pc** and **Re₁Pc** (CH_2Cl_2 , 0.1 M [*n*-Bu₄N](PF₆), vs. Fc/Fc⁺).

symmetry owing to unsymmetric coordination to the [Re(CO)₃]⁺ unit(s).

To evaluate the electrochemical properties, the cyclic voltammograms of **Re₂Pc** and **Re₁Pc** were measured (Fig. 3, Table S1). For **Re₂Pc**, one and two reversible redox waves are observed on the oxidation and reduction sides, respectively, which are typical electrochemical behaviors of the Pc ring. For **Re₁Pc**, the corresponding redox waves are observed with lower reversibility. It is noteworthy that the first oxidation potential shifts to the positive side with increasing the number of [Re(CO)₃]⁺ unit(s) in the order **ZnPc** < **Re₁Pc** < **Re₂Pc** (E^{1+0} vs. Fc/Fc⁺: +0.11 V for **ZnPc**, +0.32 V for **Re₁Pc**, and +0.52 V for **Re₂Pc**). This indicates that introduction of the [Re(CO)₃]⁺ unit(s) can not only decrease the Q-band energy, but also provide the Pc ring with tolerance to oxidation.[‡] The first and second reduction potentials also shift to the positive side with introduction of the [Re(CO)₃]⁺ unit(s). The positive shifts of the first oxidation and first reduction potentials reflect metal unit(s)-based stabilization of the HOMO and LUMO levels, respectively.⁵

To analyze the characteristic electronic properties of the Re(I) Pc complexes, theoretical calculations based on density functional theory (DFT) were performed by using the model complexes (**Re₂Pc'**, **Re₁Pc'**) with hydrogen atoms instead of *tert*-butyl groups (Fig. S5). In both optimized structures, the [Re(CO)₃]⁺ unit(s) significantly bulged from the Pc *meso*-4N plane because of the presence of three carbonyl ligands on the Re center. The nitrogen atoms of the three isoindole units were coordinated to the Re center(s). These structural features are different from the previously reported rhenium Pc complexes, in which the rhenium atom was coordinated by the Pc ligand in tetradentate mode and located in the Pc plane.¹¹ For **Re₂Pc'**, the opposite isoindole units were inclined to different sides with respect to the *meso*-4N plane, while the other two isoindole units almost laid in this plane (Fig. S6a). For **Re₁Pc'**, three coordinating isoindole units were inclined to the Re side, while the remaining unit was inclined to the other side (Fig. S6b). Thus, based on this unsymmetric coordination, the Pc rings were unusually distorted, which was clearly shown by the inclined isoindole units. Interestingly, these characteristic distortions were not the typical distortion patterns of porphyrinic compounds (saddle, waffle, dome, and wave). To confirm the structural reliability, structural optimizations were performed at

the same level for the dinuclear Re(I) tricarbonyl tetraphenylporphyrin complex (**Re₂TTP**), because Tsutsui *et al.* reported X-ray single-crystal structural analysis of **Re₂TTP**.¹³ The coordination modes of the [Re(CO)₃]⁺ unit(s), as well as the distortion pattern of **Re₂TTP**, was quite similar to that of **Re₂Pc'** (Fig. S5c, Fig. S6c, Table S2). These characteristic distortions appear in **Re₂Pc'** owing to the fused benzo units and the smaller core of the Pc ring.

Using the optimized structures of **Re₂Pc'**, **Re₁Pc'**, and non-substituted zinc(II) phthalocyanine (**ZnPc'**), molecular orbital analysis was performed (Fig. 1b, Fig. S7). For **ZnPc'** with *D*_{4h} symmetry, the HOMO is the π orbital of the Pc ring (called the a_{1u} orbital), where the pyrrolic nitrogen and *meso*-nitrogen atoms are on the nodes (no MO distribution). The degenerate LUMOs are the π^* orbitals (the e_g orbitals), where the pyrrolic carbon and nitrogen atoms, as well as the *meso*-nitrogen atoms, possess major MO distributions. For **Re₂Pc'** and **Re₁Pc'**, the HOMO and LUMO/LUMO+1 resemble those of **ZnPc'**: this indicates that the HOMO and LUMO/LUMO+1 mainly originate from the π and π^* orbitals, respectively. However, there are non-negligible HOMO distributions on the Re and pyrrolic nitrogen atoms, in addition to the LUMO/LUMO+1 distributions over the Re atom(s). This change in the HOMO distribution can be reasonably explained by structural distortion, which lowers the molecular symmetry and then the nodes disappear. Thus, because of the MO distributions over the Re and pyrrolic nitrogen atoms, both the HOMO and LUMO/LUMO+1 levels are stepwisely stabilized with increasing the number of strong electron-accepting [Re(CO)₃]⁺ units. Because the MO distributions over the Re and pyrrolic nitrogen atoms are larger in the LUMO than in the HOMO, the stabilization degree is higher in the LUMO than in the HOMO, which decreases the HOMO–LUMO gap in the order **ZnPc'** (2.18 eV) > **Re₁Pc'** (2.03 eV) > **Re₂Pc'** (1.85 eV). Furthermore, in contrast to the degenerate LUMOs of **ZnPc'**, the LUMO and LUMO+1 levels are split for **Re₁Pc'** and **Re₂Pc'** because of lowering of the symmetry of the Pc skeleton from *D*_{4h} symmetry owing to the presence of the [Re(CO)₃]⁺ units.

To further investigate the electron acceptability of the [Re(CO)₃]⁺ unit(s), atomic charges were analyzed based on natural bond orbital (NBO) and Mulliken methods (Table S3). When the Zn²⁺ center is replaced by the [Re(CO)₃]⁺ unit(s), the negative charges on the pyrrolic nitrogen and *meso*-nitrogen atoms significantly decrease. These results indicate that introduction of the electron-deficient [Re(CO)₃]⁺ unit(s) significantly reduces the electron densities of the Pc ring. This can be explained by the strong orbital interactions between the Re(I) center(s) and the pyrrolic nitrogen atoms, because the carbonyl ligands strongly enhance the π -accepting ability of the Re(I) center through π back-bonding.

Finally, TD-DFT calculations were performed to analyze the excited-state properties (Fig. 2c, Table S4). Although the calculated transition energies were higher than the experimentally determined values, the simulated spectra well reproduced the observed spectra in terms of the lower energy shift and the splitting of the Q band owing to the [Re(CO)₃]⁺ unit. For the lowest excited singlet states, the calculated transition

energies shifted to the lower energy side in the order \mathbf{ZnPc}^* (1.997 and 1.997 eV) > $\mathbf{Re}_1\mathbf{Pc}^*$ (1.816 and 1.819 eV) > $\mathbf{Re}_2\mathbf{Pc}^*$ (1.640 and 1.691 eV). The S_{1x} and S_{1y} states, which mainly originate from HOMO (π) \rightarrow LUMO (π^*) and HOMO (π) \rightarrow LUMO+1 (π^*) transitions, respectively, are degenerate for \mathbf{ZnPc}^* . However, the degeneracy between the S_{1x} and S_{1y} states is lifted for $\mathbf{Re}_2\mathbf{Pc}^*$ (0.003 eV) and $\mathbf{Re}_1\mathbf{Pc}^*$ (0.051 eV). These calculated results are consistent with experimental observations, such as the broadening of the Q band and the MCD quasi-Faraday A term. The MLCT transitions (d_π (Re) \rightarrow e_g (Pc)) contribute to the S_{1x} and S_{1y} states (Table S4), which is also considered to be one of the factors that lowers the energy levels of the S_{1x} and S_{1y} states.

In conclusion, we have successfully developed novel Re(I) Pc complexes that are stable and show intense absorption bands in the NIR region. The remarkable lowering of the Q-band energy and the improvement of tolerance to oxidation are concomitantly realized by simple modification of the central metal. Incorporation of the electron-deficient $[\text{Re}(\text{CO})_3]^+$ unit(s) stabilizes both the HOMO and LUMO levels. On the basis of the MO distribution on the pyrrolic nitrogen atoms, stabilization of the LUMO level is larger than that of the HOMO level, which reduces the HOMO–LUMO gap. In particular, the abnormal distortion of the Pc ring owing to coordination of the $[\text{Re}(\text{CO})_3]^+$ unit(s) provides the HOMO distribution on the pyrrolic nitrogen atoms and HOMO stabilization, which increase the tolerance to oxidation. The present strategy is considered to be promising for simple reasonable design of Pc-based NIR absorbers with high tolerance to oxidation, which can be used for various applications, such as photofunctional materials.

K.I. acknowledges support from JSPS KAKENHI (grant number JP17H06375). K.M. acknowledges support from JSPS KAKENHI (grant number JP19K15582) and JST, ACT-X (grant number JPMJAX191H), Japan. The DFT computations were performed using Research Center for Computational Science (Okazaki, Japan).

Conflicts of interest

There are no conflicts to declare.

Notes and references

‡ The effect of $[\text{Re}(\text{CO})_3]^+$ unit(s) on the tolerance to oxidation was examined by monitoring the decomposition of the Pc ring due to singlet oxygen (Fig. S4 in ESI).

- (a) B. D. Ravetz, A. B. Pun, E. M. Churchill, D. N. Congreve, T. Rovis and L. M. Campos, *Nature*, 2019, **565**, 343–346; (b) G. de la Torre, C. G. Claessens and T. Torres, *Chem. Commun.*, 2007, 2000–2015; (c) M. K. Panda, K. Ladomenou and A. G. Coutsolelos, *Coord. Chem. Rev.*, 2012, **256**, 2601–2627; (d) M.-E. Ragoussi, M. Ince and T. Torres, *Eur. J. Org. Chem.*, 2013, 6475–6489; (e) L. Martín-Gomis, F. Fernández-Lázaro and Á. Sastre-Santos, *J. Mater. Chem. A*, 2014, **2**, 15672–15682; (f) H. Imahori, in *Handbook of Porphyrin Science*; ed. K. M. Kadish, K. M. Smith and R. Guilard, World Scientific Pub Co Inc, 2012, Vol. 18, pp. 57–121.
- (a) J. G. Moser, *Photodynamic Tumor Therapy: 2nd and 3rd Generation Photosensitizers*, Harwood Academic Publishers, Amsterdam, 1998; (b) T. Patrice, *Photodynamic Therapy*, The Royal

- (a) K. Ishii, M. Shiine, Y. Shimizu, S. Hoshino, H. Abe, K. Sogawa and N. Kobayashi, *J. Phys. Chem. B*, 2008, **112**, 3138–3143; (d) T. Yokoi, T. Otani and K. Ishii, *Sci. Rep.*, 2018, **8**, 1560; (e) T. C. Gunaratne, A. V. Gusev, X. Peng, A. Rosa, G. Ricciardi, E. J. Baerends, C. Rizzoli, M. E. Kenney and M. A. J. Rodgers, *J. Phys. Chem. A*, 2005, **109**, 2078–2089.
- (a) T. Hoshi and N. Kobayashi, *Coord. Chem. Rev.*, 2017, **345**, 31–41; (b) Y. Rio, M. S. Rodríguez-Morgade and T. Torres, *Org. Biomol. Chem.*, 2008, **6**, 1877–1894; (c) N. Kobayashi and H. Konami, in *Phthalocyanines-Properties and Applications*; ed. C. C. Leznoff and A. B. P. Lever, VCH, New York, 1996, Vol. 4, Chapter 9.
- N. Kobayashi, S. Nakajima, H. Ogata and T. Fukuda, *Chem. Eur. J.*, 2004, **10**, 6294–6312.
- (a) H. Miwa, K. Ishii and N. Kobayashi, *Chem. Eur. J.*, 2004, **10**, 4422–4435; (b) N. Kobayashi, J. Mack, K. Ishii and M. J. Stillman, *Inorg. Chem.*, 2002, **41**, 5350–5363; (c) N. Kobayashi, H. Miwa and V. N. Nemykin, *J. Am. Chem. Soc.*, 2002, **124**, 8007–8020; (d) N. Kobayashi and T. Fukuda, *J. Am. Chem. Soc.*, 2002, **124**, 8021–8034; (e) J. Mack and N. Kobayashi, *Chem. Rev.*, 2011, **111**, 281–321; (f) E. W. Y. Wong, A. Miura, M. D. Wright, Q. He, C. J. Walsby, S. Shimizu, N. Kobayashi and D. B. Leznoff, *Chem. Eur. J.*, 2012, **18**, 12404–12410.
- (a) N. Kobayashi, H. Ogata, N. Nonaka and E. A. Luk'yanets, *Chem. Eur. J.*, 2003, **9**, 5123–5134; (b) P. M. Burnham, M. J. Cook, L. A. Gerrard, M. J. Heaney and D. L. Hughes, *Chem. Commun.*, 2003, 2064–2065; (c) S. Z. Topal, Ü. İsci, U. Kumru, D. Atilla, A. G. Gürek, C. Hirel, M. Durmuş, J.-B. Tommasino, D. Luneau, S. Berber, F. Dumoulin and V. Ahsen, *Dalton Trans.*, 2014, **43**, 6897–6908.
- (a) N. Kobayashi, T. Fukuda, K. Ueno and H. Ogino, *J. Am. Chem. Soc.*, 2001, **123**, 10740–10741; (b) H. Ryeng and A. Ghosh, *J. Am. Chem. Soc.*, 2002, **124**, 8099–8103.
- U. Michelsen, G. Schnurpfeil, A. K. Sobbi, D. Wöhrle and H. Kliesch, *Photochem. Photobiol.*, 1996, **64**, 694–701.
- (a) O. V. Dolotova, N. I. Bundina, O. L. Kaliya and E. A. Lukyanets, *J. Porphyrins Phthalocyanines*, 1997, **1**, 355–366; (b) C. C. Leznoff, L. S. Black, A. Hiebert, P. W. Causey, D. Christendat and A. B. P. Lever, *Inorg. Chim. Acta*, 2006, **359**, 2690–2699; (c) G. Mbambisa, P. Tau, E. Antunes and T. Nyokong, *Polyhedron*, 2007, **26**, 5355–5364; (d) D. McKearney, W. Zhou, C. Zellman, V. E. Williams and D. B. Leznoff, *Chem. Commun.*, 2019, **55**, 6696–6699.
- (a) J. P. Fox and D. P. Goldberg, *Inorg. Chem.*, 2003, **42**, 8181–8191; (b) N. Kobayashi, T. Furuyama and K. Satoh, *J. Am. Chem. Soc.*, 2011, **133**, 19642–19645; (c) T. Furuyama, K. Satoh, T. Kushiya and N. Kobayashi, *J. Am. Chem. Soc.*, 2014, **136**, 765–776; (d) T. Fukuda, K. Ono, S. Homma and N. Kobayashi, *Chem. Lett.*, 2003, 736–737.
- (a) W. Darwish, E. Seikel, K. Harms, O. Burghaus, J. Sundermeyer, *Dalton Trans.*, 2011, **40**, 1183–1188.; (b) S. Verma, M. Hanack, *Z. Anorg. Allg. Chem.*, 2003, **629**, 880–892.; (c) M. GoEldnera, B. Geniffkea, A. Frankena, K. S. Murraybund, H. Homborg, *Z. Anorg. Allg. Chem.*, 2001, **627**, 935–947.; (d) K. Frick, S. Verma, J. Sundermeyer, M. Hanack, *Eur. J. Inorg. Chem.*, 2000, 1025–1030.
- (a) W. R. Browett and M. J. Stillman, *Comput. Chem.*, 1987, **11**, 241–250; (b) J. Mack and M. J. Stillman, in *The Porphyrin Handbook*, ed. K. M. Kadish, R. M. Smith and R. Guilard, Academic Press, New York, 2003, Vol. 16, Chapter 103; (c) M. J. Stillman and T. Nyokong, in *Phthalocyanines-Properties and Applications*, ed. C. C. Leznoff and A. B. P. Lever, VCH, New York, 1989, Vol. 1, Chapter 3; (d) M. J. Stillman, in *Phthalocyanines-Properties and Applications*, ed. C. C. Leznoff and A. B. P. Lever, VCH, New York, 1993, Vol. 3, Chapter 5; (e) J. Mack and M. J. Stillman, *Coord. Chem. Rev.*, 2001, **219–221**, 993–1032.
- (a) D. Ostfeld, M. Tsutsui, C. P. Hsung and D. C. Conway, *J. Coord. Chem.*, 1972, **2**, 101–106; (b) M. Tsutsui, C. P. Hsung, D. Ostfeld, T. S. Srivastava, D. L. Cullen and E. F. Meyer Jr., *J. Am. Chem. Soc.*, 1975, **97**, 3952–3965.

TOC Unsymmetric coordination of the electron-deficient Re(I) unit(s) to the phthalocyanine ring concomitantly realized the intense absorption in near-infrared region and the improvement of tolerance to oxidation.

